Organic LETTERS

Letter

pubs.acs.org/OrgLett

Mechanism and Stereoselectivity in an Asymmetric N-Heterocyclic Carbene-Catalyzed Carbon−Carbon Bond Activation Reaction

Monika Pareek and Raghavan B. Sunoj*

Department of Chemistry, Indian Institute of Technology Bombay, Powai, Mumbai 400076, India

Supporting Information

ABSTRACT: The mechanism and origin of stereoinduction in a chiral N-heterocyclic carbene (NHC) catalyzed C−C bond activation of cyclobutenone has been established using B3LYP-D3 density functional theory computations. The activation of cyclobutenone as an NHC-bound vinyl enolate and subsequent reaction with the electrophilic sulfonyl imine leads to the lactam product. The most preferred stereocontrolling transition state exhibits a number of noncovalent interactions rendering additional stabilization. The computed enantio- and diastereoselectivities are in good agreement with the previous experimental observations.

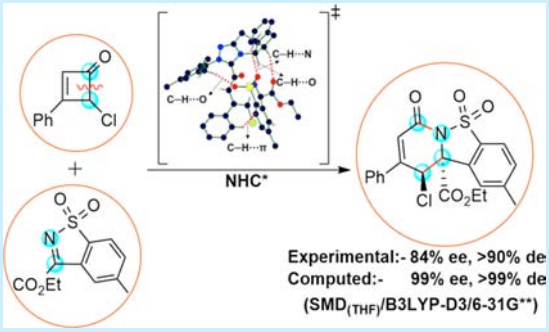

N-heterocyclic carbenes (NHCs) have emerged as an efficient organocatalyst for asymmetric applications in recent years.[1] In most of the catalytic applications, NHC renders umpolung reactivity to aldehydes and ketones through the formation of acyl anion equivalent,[2] homoenolate,[3] enolate,[4] or α-acylvinyl anion equivalent.[5] An impressive array of asymmetric reactions such as annulation, benzoin, Stetter, Mannich, Michael, Claisen rearrangement, and cycloaddition are indeed a testimony to its versatility as an organocatalyst.[6] The foray of NHCs into the domain of transition-metal catalysis are equally impressive where its function is largely as a ligand to the transition metals.[7] Most recent organocatalytic applications of NHCs appear to expand its repertoire even to the fortress of transition-metal catalysis. Similar efforts in NHC catalysis have been extended to C−H bond[8] and C−C bond activations.[9] It is conspicuous that catalytic activation of carbon−carbon and carbon−hydrogen single bonds can provide direct access to useful functionalized molecules.

While NHC catalysis generally banks on the activation of aldehydes in the form of Breslow intermediates,[1,10] studies aimed at exploiting ketone as a substrate are far fewer.[11] Recently, Chi and co-workers reported the activation of the C−C bond using chiral bicyclic triazolium NHCs as organocatalyst.[9] Through this interesting catalytic route, chiral lactams could be synthesized in a redox-neutral and atom-economic manner. Even though there have been proposed mechanisms and transition-state models for NHC-catalyzed asymmetric reactions,[12] its role in C−C bond activation is not yet established. In the present study, we present important mechanistic insights into the C−C bond activation and the origin of stereoselectivity in the reaction between cyclobutenone and sulfonyl imines (Scheme 1), as obtained using the $SMD_{(THF)}$/B3LYP-D3/6-31G** computational methods. The discussions are presented on the basis of the Gibbs free energies of reactants, intermediates, and transition states (TS).[13]

Scheme 1. Reaction between Cyclobutenone and Sulfonyl Imine Catalyzed by Chiral NHC to form Lactam Product

The important mechanistic events are shown in Scheme 2. The generation of the free NHC from the catalyst precursor can be considered as taking place by the action of cesium carbonate, wherein the latter deprotonates the triazolium moiety. The active carbene can then participate in the catalytic cycle through its reaction with the unsaturated four-membered cyclic ketone to generate zwitterionic intermediate **2**. In the subsequent step, the ring-opening of cyclic butenone through the C−C bond breaking leads to the formation of chiral NHC-tethered vinyl enolate intermediate **3**. The next important step is the stereoselective C−C bond formation between the nucleophilic vinyl enolate **3** and the electrophilic sulfonyl imine **4**. In the ensuing step, an intramolecular nucleophilic addition of the sulfonamidate nitrogen to the carbonyl carbon takes place to form intermediate **6**. In the final step of the catalytic cycle, the expulsion of NHC provides the desired six-membered lactam product **7**.[14]

Each step described in the overall catalytic cycle, as given in Scheme 2, is examined in greater detail to identify the energetically most preferred pathway. The different possibilities are considered for the initial nucleophilic addition of the chiral NHC to cyclobutenone **1**. These possibilities arise due to the approach of (i) the NHC to different prochiral faces of **1** and (ii) the differences in the dihedral angle along the incipient C−C

Received: October 10, 2016
Published: November 9, 2016

DOI: 10.1021/acs.orglett.6b03043
Org. Lett. 2016, 18, 5932−5935

Scheme 2. Key Mechanistic Steps Involved in Chiral NHC-Catalyzed C−C Bond Activation of Cyclobutenone

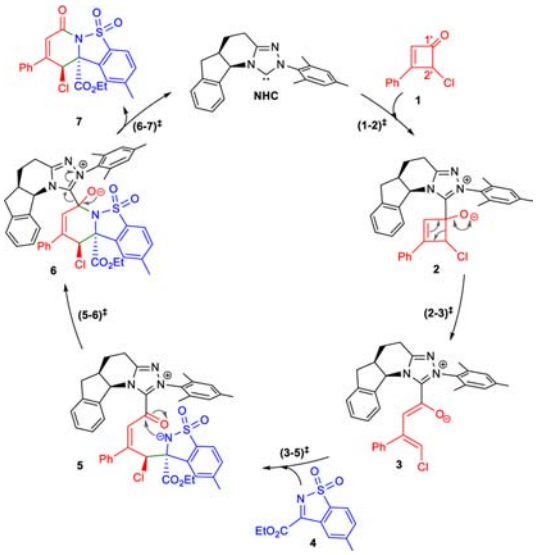

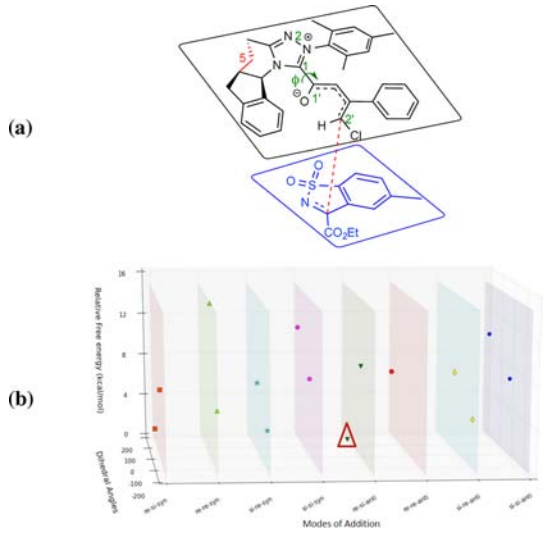

Figure 1. (a) Conformational analysis using O1′−C1′−C1−N2 dihedral angle. (b) Stereochemical possibilities for the C−C bond formation and the corresponding Gibbs free energy (in kcal/mol) distribution conformers.

bond.[15] The addition of NHC to the *re* face of cyclobutenone is found to be the most preferred mode. The NHC addition to cyclobutenone disturbs the conjugation of the α,β-unsaturated ketone and results in weakening of the C1′−C2′ bond in the ensuing intermediate **2**.[16] The longer C1′−C2′ bond lowers the ring strain in cyclobutenone and triggers the generation of the vinyl enolate intermediate **3**.

The next step involves the stereoselective C−C bond formation between the vinyl enolate **3** and sulfonyl imine (**4**). This is the most vital step of the reaction that dictates the stereochemical outcome. Hence, we have carefully examined various stereochemical modes of approach between the electrophilic and nucleophilic reacting partners. The key differences between such possibilities are in terms of the *re* or *si* prochiral faces involved in the C−C bond formation and in the ring conformation of the C5 methylene group of the triazole fused six-membered ring, as shown in Figure 1. The CH_2 group can either remain in a *syn* relative orientation toward the indan ring or can be in an *anti* position opposite to the indan ring. Other conformational possibilities arising due to the orientation of the vinyl enolate oxygen toward or away from the mesityl group are also examined.[17]

A total of 16 transition states (TSs) have been considered. The range of Gibbs free energies of these TSs can be gleaned from Figure 1b. These TSs are grouped together in eight vertical planes comprising *syn* and *anti* ring conformers besides the differences in the prochiral faces involved in the C−C bond formation and in the orientation of the vinyl enolate. After careful consideration of C−C bond formation TSs involving different prochiral faces of vinyl enolate and sulfonyl imine, we could identify that the nucleophilic addition of the *re* face of vinyl enolate to the *si* face of the sulfonyl imine (when the C5 methylene is in an *anti* orientation) is the lowest energy mode. The *re-si* mode will result in the formation of two new stereocenters with 10*S*,10a*R* configuration (Scheme 1). The TS for the *si-re* mode of addition is found to be 3.8 kcal/mol higher and corresponds to an enantiomeric excess of 99.7%. Similarly, the *re-re* addition TS for the formation of the diastereomeric product is 6.0 kcal/mol higher in energy than the most preferred *re-si* mode, suggesting a diastereomeric excess of >99.0%.

The predicted stereoselectivities are in accordance with experimental observations. It is gratifying to note that the computed lowest energy $(\mathbf{3-5})_{re\text{-}si}^{\ddagger}$ corresponds to the experimentally observed major stereoisomer with 10*S*,10a*R* configuration. Having predicted the correct stereochemical outcome of the reaction, we turned our attention toward deciphering the origin of preference for the *re-si* mode of addition over all other modes. To rationalize the energy difference between $(\mathbf{3-5})_{re\text{-}si}^{\ddagger}$ and $(\mathbf{3-5})_{si\text{-}re}^{\ddagger}$, the stereoelectronic features are carefully analyzed. Widely employed approaches based on the topological distribution of electron density, such as the atoms in molecule (AIM)[18] and noncovalent interaction (NCI) plot,[19] have been used. In both these methods, the interactions between atoms/groups as well as the regions of attractive and repulsive interactions can be identified. The presence of a bond critical point between a pair of atoms is generally considered as an indicator of an interatomic interaction in the AIM formalism and the value of electron density at such bond critical points (ρ_{bcp}) corresponds to the strength of interaction. In Figure 2, ρ_{bcp} values are provided in parentheses beside the respective interatomic distances.

In the lower energy $(\mathbf{3-5})_{re\text{-}si}^{\ddagger}$, the C−H···O interaction between the mesityl methyl and the sulfonyl oxygen (depicted as (a) in Figures 2 and 3), the C−H···π interaction between the phenyl (of the enolate) and the benzothiazole ring (b), and the lone pair···π interaction between sulfonyl oxygen and the vinyl group (c) are found to be relatively stronger than the corresponding interactions in the diastereomeric $(\mathbf{3-5})_{si\text{-}re}^{\ddagger}$. A C−H···N interaction between the indan hydrogen and the imino nitrogen of the heterocyclic ring (e) is noticed in $(\mathbf{3-5})_{re\text{-}si}^{\ddagger}$ but not in $(\mathbf{3-5})_{si\text{-}re}^{\ddagger}$. In recent years, the origin of stereoselectivity in many asymmetric transformations has increasingly been suggested as controlled by noncovalent interactions.[20] The C5 methylene group of the triazole fused ring is found to participate in noncovalent interactions, depending on whether it is in a *syn* and *anti* orientation with respect to the indan ring. The C−H···O interaction is present in $(\mathbf{3-5})_{re\text{-}si}^{\ddagger}$, when the C5 methylene

DOI: 10.1021/acs.orglett.6b03043
Org. Lett. 2016, 18, 5932−5935

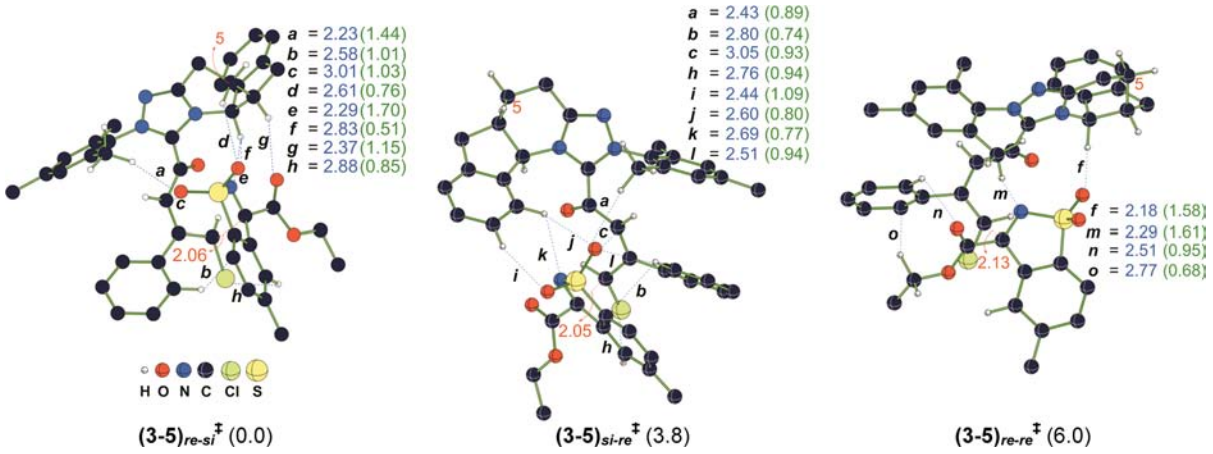

Figure 2. Important transition states for the C−C bond formation between the vinyl enolate and sulfonyl imine and the corresponding relative Gibbs free energies (in kcal/mol) at the $SMD_{(THF)}$/B3LYP-D3/6-31G** level of theory. Distances (Å) and the electron densities ($\rho \times 10^{-2}$ au) at the bond critical points (in parentheses) are given. The red dotted lines represent the reaction coordinate. Only select hydrogen atoms are shown.

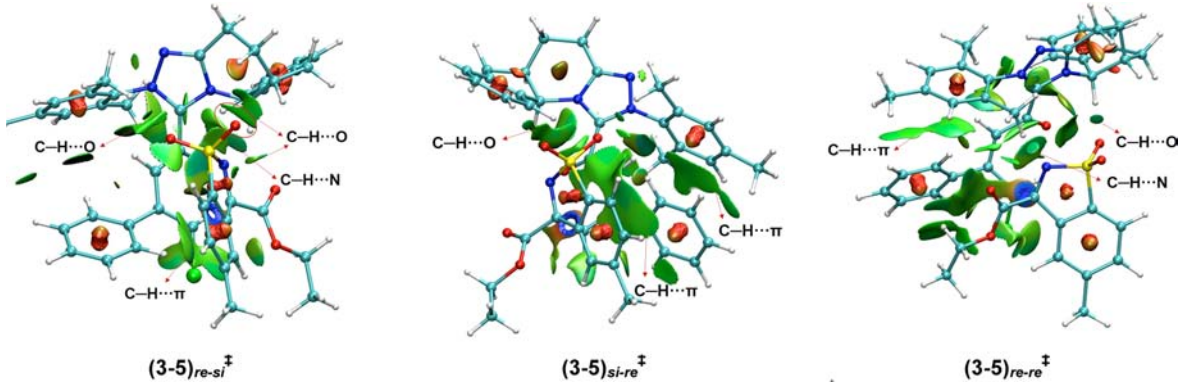

Figure 3. Noncovalent interaction (NCI) plot for the C−C bond formation transition states [$(3-5)^{‡}$]. The green, blue and red regions respectively represent attractive, strongly attractive and repulsive interactions.

group is *anti* to the indan ring. When the C5 methylene is *syn*, such interaction is absent as shown in Figure 2.

The analysis of NCI plots has given interesting molecular insights on the stereocontrolling TSs (Figure 3). In a NCI plot, the regions of attractive noncovalent interactions appear as green color regions, while red regions represent repulsive interactions. It can be readily noticed that the noncovalent interactions are more prominent in the lowest energy $(3-5)_{re\text{-}si}^{‡}$. The number of C−H···O interactions is more in $(3-5)_{re-si}^{‡}$ than in the higher energy $(3-5)_{si\text{-}re}^{‡}$ as noticeable from a relatively larger area of the green color region. The C−H···N interaction in $(3-5)_{re\text{-}si}^{‡}$ is evidently absent in other diastereomeric TSs. All these additional interactions as well as the relatively better efficiency in the common interactions together contribute to the stabilization of $(3-5)_{re\text{-}si}^{‡}$.

Further analysis of the stereocontrolling TSs is performed by using the activation strain model.[21] The contribution to the activation energy arising from the destabilizing distortions of the reactants (the energy difference between the distorted geometry of the reactants in the TS and that of the undistorted ground state) and the stabilizing interaction between the distorted reactants in the TSs are calculated.[22] The distortion energy and interaction energy are more in the most preferred $(3-5)_{re\text{-}si}^{‡}$ than in the higher energy $(3-5)_{si\text{-}re}^{‡}$, which is in line with an energy difference of 3.8 kcal/mol between these two TSs. The reacting components, i.e., vinyl enolate and sulfonylimine, appear to get more distorted in $(3-5)_{re\text{-}si}^{‡}$ so as to maximize the interaction between the distorted fragments.

After having analyzed the energetic origin of high stereoselectivity imparted in the C−C bond formation step, we have examined the overall energetic features of the catalytic cycle. It is evident from the Gibbs free energy profile given in Figure 4 that

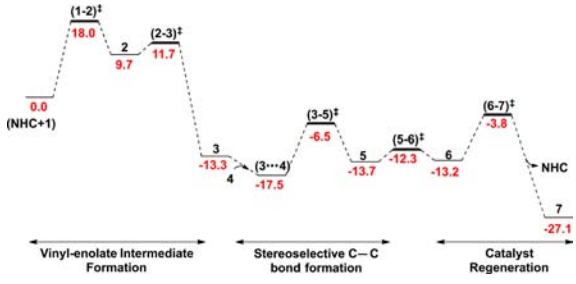

Figure 4. Gibbs free energy profile (kcal/mol) for the formation of lactam at the $SMD_{(THF)}$/B3LYP-D3/6-31G** level of theory.

the initial nucleophilic addition of the chiral NHC to the cyclobutenone is of the highest activation barrier. The most interesting aspect relates to the C−C bond activation step wherein a higher energy adduct (**2**) (formed between the NHC and cyclobutenone) prefers to move forward to vinyl enolate **3**. The exoergic formation of **3** can be attributed to the relieving of the ring strain in intermediate **2**. An additional impetus in the

DOI: 10.1021/acs.orglett.6b03043
Org. Lett. 2016, 18, 5932−5935

form of formation of a prereacting complex (**3**···**4**) between vinyl enolate and sulfonylimine is also noticeable.[23] All other steps are quite feasible in the catalytic cycle. The activation barrier associated with the stereocontrolling $(\mathbf{3}-\mathbf{5})_{re\text{-}si}^{\ddagger}$ is 11 kcal/mol. The formation of final annulated product **7** is exergonic by more than 27 kcal/mol, indicating a thermodynamic drive for this reaction and for the release of the free NHC for the catalytic cycle to sustain.

In conclusion, the energetically preferred pathway in the reaction between cyclobutenone and sulfonylimine toward the formation of chiral lactam has been identified. The activation of cyclobutenone by the action of chiral NHC leads to a vinyl enolate intermediate, the *re* prochiral face of which then adds to the *si* face of sulfonylimine in the stereocontrolling C−C bond formation. The stereochemical preference for the *re-si* addition leading to 10*S*,10a*R* as the major product is traced to the presence of relatively more efficient noncovalent interactions (C−H···O, C−H···π, lone pair···π) in the lower energy transition state.

■ ASSOCIATED CONTENT

Supporting Information

The Supporting Information is available free of charge on the ACS Publications website at DOI: 10.1021/acs.orglett.6b03043.

Optimized geometries, details of conformational analyses, AIM and NBO data, and Cartesian coordinates (PDF)

■ AUTHOR INFORMATION

Corresponding Author

*E-mail: sunoj@chem.iitb.ac.in

Notes

The authors declare no competing financial interest.

■ ACKNOWLEDGMENTS

Computing time from IIT Bombay supercomputing and a senior research fellowship from CSIR-New Delhi (M.P.) are acknowledged.

■ REFERENCES

(1) (a) Flanigan, D. M.; Romanov-Michailidis, F.; White, N. A.; Rovis, T. *Chem. Rev.* **2015**, *115*, 9307. (b) Hopkinson, M. N.; Richter, C.; Schedler, M.; Glorius, F. *Nature* **2014**, *510*, 485. (c) Ryan, S. J.; Candish, L.; Lupton, D. W. *Chem. Soc. Rev.* **2013**, *42*, 4906. (d) Bugaut, X.; Glorius, F. *Chem. Soc. Rev.* **2012**, *41*, 3511.

(2) (a) Kerr, M. S.; Read de Alaniz, J.; Rovis, T. *J. Am. Chem. Soc.* **2002**, *124*, 10298. (b) Menon, R. S.; Biju, A. T.; Nair, V. *Chem. Soc. Rev.* **2015**, *44*, 5040.

(3) (a) Burstein, C.; Glorius, F. *Angew. Chem., Int. Ed.* **2004**, *43*, 6205. (b) Chan, A.; Scheidt, K. A. *Org. Lett.* **2005**, *7*, 905. (c) Sohn, S. S.; Rosen, E. L.; Bode, J. W. *J. Am. Chem. Soc.* **2004**, *126*, 14370. (d) Nair, V.; Vellalath, S.; Poonoth, M.; Suresh, E. *J. Am. Chem. Soc.* **2006**, *128*, 8736.

(4) (a) Wadamoto, M.; Phillips, E. M.; Reynolds, T. E.; Scheidt, K. A. *J. Am. Chem. Soc.* **2007**, *129*, 10098. (b) Reynolds, N. T.; Rovis, T. *J. Am. Chem. Soc.* **2005**, *127*, 16406. (c) He, M.; Uc, G. J.; Bode, J. W. *J. Am. Chem. Soc.* **2006**, *128*, 15088.

(5) Reynolds, T. E.; Stern, C. A.; Scheidt, K. A. *Org. Lett.* **2007**, *9*, 2581.

(6) (a) Jousseaume, T.; Wurz, N. E.; Glorius, F. *Angew. Chem., Int. Ed.* **2011**, *50*, 1410. (b) DiRocco, D. A.; Rovis, T. *J. Am. Chem. Soc.* **2011**, *133*, 1040. (c) Enders, D.; Grossmann, A.; Fronert, J.; Raabe, G. *Chem. Commun.* **2010**, *46*, 6282. (d) Ryan, S. J.; Candish, L.; Lupton, D. W. *J. Am. Chem. Soc.* **2011**, *133*, 4694. (e) Kaeobamrung, J.; Kozlowski, M. C.; Bode, J. W. *Proc. Natl. Acad. Sci. U. S. A.* **2010**, *107*, 20661.

(7) (a) Hahn, F. E.; Jahnke, M. C. *Angew. Chem., Int. Ed.* **2008**, *47*, 3122. (b) Lin, J. C. Y.; Roy, T.; Huang, W.; Lee, C. S.; Bhattacharyya, A.; Hwang, W. S.; Lin, I. J. B. *Chem. Rev.* **2009**, *109*, 3561. (c) Würtz, S.; Glorius, F. *Acc. Chem. Res.* **2008**, *41*, 1523.

(8) (a) Fu, Z.; Xu, J.; Zhu, T.; Leong, W. W. Y.; Chi, Y. R. *Nat. Chem.* **2013**, *5*, 835. (b) Reddi, Y.; Sunoj, R. B. *ACS Catal.* **2015**, *5*, 5794.

(9) (a) Li, B.-S.; Wang, Y.; Jin, Z.; Zheng, P.; Ganguly, R.; Chi, Y. R. *Nat. Commun.* **2015**, *6*, 6207. (b) Li, B.-S.; Wang, Y.; Jina, Z.; Chi, Y. R. *Chem. Sci.* **2015**, *6*, 6008.

(10) (a) Berkessel, A.; Yatham, V. R.; Elfert, S.; Neudörfl, J.-M. *Angew. Chem., Int. Ed.* **2013**, *52*, 11158. (b) Paul, M.; Breugst, M.; Neudörfl, J.-M.; Sunoj, R. B.; Berkessel, A. *J. Am. Chem. Soc.* **2016**, *138*, 5044.

(11) (a) Chiang, P.-C.; Rommel, M.; Bode, J. W. *J. Am. Chem. Soc.* **2009**, *131*, 8714. (b) Binanzer, M.; Hsieh, S.-Y.; Bode, J. W. *J. Am. Chem. Soc.* **2011**, *133*, 19698.

(12) (a) DiRocco, D. A.; Noey, E. L.; Houk, K. N.; Rovis, T. *Angew. Chem., Int. Ed.* **2012**, *51*, 2391. (b) Reddi, Y.; Sunoj, R. B. *Org. Lett.* **2012**, *14*, 2810. (c) Lyngvi, E.; Bode, J. W.; Schoenebeck, F. *Chem. Sci.* **2012**, *3*, 2346. (d) Pareek, M.; Sunoj, R. B. *ACS Catal.* **2016**, *6*, 3118. (e) Reddi, Y.; Sunoj, R. B. *ACS Catal.* **2015**, *5*, 1596. (f) Wang, Y.; Wu, B.; Zhang, H.; Wei, D.; Tang, M. *Phys. Chem. Chem. Phys.* **2016**, *18*, 19933.

(13) *Gaussian 09*, Revision D.01: Frisch, M. J.; Trucks, G. W.; Schlegel, H. B.; Scuseria, G. E.; Robb, M. A.; Cheeseman, J. R.; Scalmani, G.; Barone, V.; Mennucci, B.; Petersson, G. A.; Nakatsuji, H.; Caricato, M.; Li, X.; Hratchian, H. P.; Izmaylov, A. F.; Bloino, J.; Zheng, G.; Sonnenberg, J. L.; Hada, M.; Ehara, M.; Toyota, K.; Fukuda, R.; Hasegawa, J.; Ishida, M.; Nakajima, T.; Honda, Y.; Kitao, O.; Nakai, H.; Vreven, T.; Montgomery, J. A., Jr.; Peralta, J. E.; Ogliaro, F.; Bearpark, M.; Heyd, J. J.; Brothers, E.; Kudin, K. N.; Staroverov, V. N.; Kobayashi, R.; Normand, J.; Raghavachari, K.; Rendell, A.; Burant, J. C.; Iyengar, S. S.; Tomasi, J.; Cossi, M.; Rega, N.; Millam, N. J.; Klene, M.; Knox, J. E.; Cross, J. B.; Bakken, V.; Adamo, C.; Jaramillo, J.; Gomperts, R.; Stratmann, R. E.; Yazyev, O.; Austin, A. J.; Cammi, R.; Pomelli, C.; Ochterski, J. W.; Martin, R. L.; Morokuma, K.; Zakrzewski, V. G.; Voth, G. A.; Salvador, P.; Dannenberg, J. J.; Dapprich, S.; Daniels, A. D.; Farkas, O.; Foresman, J. B.; Ortiz, J. V.; Cioslowski, J.; Fox, D. J. Gaussian, Inc.: Wallingford, CT, 2013.

(14) The δ lactam core is an important precursor for many biological active compounds. Popham, D. L.; Helin, J.; Costello, C. E.; Setlow, P. *Proc. Natl. Acad. Sci. U. S. A.* **1996**, *93*, 15405.

(15) See Table S1 and Figure S1 in the Supporting Information.

(16) (a) The NBO analysis revealed that the lone pair from the enolate oxygen gets delocalized into the C1′−C2′ antibonding orbital, leading to weakening of the bond.. (b) The details of the NBO analysis are provided in Table S2 in the Supporting Information.

(17) See Figure S2 and Table S3 in the Supporting Information.

(18) (a) Bader, R. F. W. *Chem. Rev.* **1991**, *91*, 893. (b) AIM2000 Version 2.0; *Buro fur Innovative Software*, SBK-Software: Bielefeld, 2002. (c) Details of AIM analysis are provided in Figure S3 and Table S4 in the Supporting Information.

(19) (a) Johnson, E. R.; Keinan, S.; Mori-Sanchez, P.; Contreras-García, J.; Cohen, A. J.; Yang, W. *J. Am. Chem. Soc.* **2010**, *132*, 6498. (b) Contreras-García, J.; Johnson, E. R.; Keinan, S.; Chaudret, R.; Piquemal, J.-P.; Beratan, D. N.; Yang, W. *J. Chem. Theory Comput.* **2011**, *7*, 625.

(20) (a) Sunoj, R. B. *Acc. Chem. Res.* **2016**, *49*, 1019. (b) Uyeda, C.; Jacobsen, E. N. *J. Am. Chem. Soc.* **2011**, *133*, 5062. (c) Johnston, R. C.; Cheong, P. H.-Y. *Org. Biomol. Chem.* **2013**, *11*, 5057. (d) Allen, S. E.; Mahatthananchai, J.; Bode, J. W.; Kozlowski, M. C. *J. Am. Chem. Soc.* **2012**, *134*, 12098. (e) Wheeler, S. E.; Seguin, T. J.; Guan, Y.; Doney, A. C. *Acc. Chem. Res.* **2016**, *49*, 1061.

(21) (a) Bickelhaupt, F. M. *J. Comput. Chem.* **1999**, *20*, 114. (b) van Zeist, W.-J.; Bickelhaupt, F. M. *Org. Biomol. Chem.* **2010**, *8*, 3118.

(22) See Table S5 in the Supporting Information.

(23) The C−H···O and C−H···N interactions between sulfonyl imine and intermediate **3** results in additional stabilization of intermediate **3**···**4** as noted in the energy profile.

DOI: 10.1021/acs.orglett.6b03043
Org. Lett. 2016, 18, 5932−5935